Sensitivity of point scale surface runoff predictions to rainfall resolution

A. J. Hearman, C. Hinz

Hydrol. Earth Syst. Sci., 11, 965–982, 2007
www.hydrol-earth-syst-sci.net/11/965/2007/

Hydrology and Earth System Sciences

Sensitivity of point scale surface runoff predictions to rainfall resolution

A. J. Hearman and C. Hinz

School of Earth and Geographical Sciences, The University of Western Australia, Crawley, Australia

Received: 10 October 2006 – Published in Hydrol. Earth Syst. Sci. Discuss.: 17 November 2006
Revised: 13 February 2007 – Accepted: 21 February 2007 – Published: 5 March 2007

Abstract. This paper investigates the effects of using non-linear, high resolution rainfall, compared to time averaged rainfall on the triggering of hydrologic thresholds and therefore model predictions of infiltration excess and saturation excess runoff at the point scale. The bounded random cascade model, parameterized to three locations in Western Australia, was used to scale rainfall intensities at various time resolutions ranging from 1.875 min to 2 h. A one dimensional, conceptual rainfall partitioning model was used that instantaneously partitioned water into infiltration excess, infiltration, storage, deep drainage, saturation excess and surface runoff, where the fluxes into and out of the soil store were controlled by thresholds. The results of the numerical modelling were scaled by relating soil infiltration properties to soil draining properties, and in turn, relating these to average storm intensities. For all soil types, we related maximum infiltration capacities to average storm intensities (k^*) and were able to show where model predictions of infiltration excess were most sensitive to rainfall resolution ($\ln k^*=0.4$) and where using time averaged rainfall data can lead to an under prediction of infiltration excess and an over prediction of the amount of water entering the soil ($\ln k^*>2$) for all three rainfall locations tested. For soils susceptible to both infiltration excess and saturation excess, total runoff sensitivity was scaled by relating drainage coefficients to average storm intensities (g^*) and parameter ranges where predicted runoff was dominated by infiltration excess or saturation excess depending on the resolution of rainfall data were determined ($\ln g^*<2$). Infiltration excess predicted from high resolution rainfall was short and intense, whereas saturation excess produced from low resolution rainfall was more constant and less intense. This has important implications for the accuracy of current hydrological models that use time averaged rainfall under these soil and rainfall conditions and predictions of larger scale phenomena such as hillslope runoff and runon. It offers insight into how rainfall resolution can affect predicted amounts of water entering the soil and thus soil water storage and drainage, possibly changing our understanding of the ecological functioning of the system or predictions of agrichemical leaching. The application of this sensitivity analysis to different rainfall regions in Western Australia showed that locations in the tropics with higher intensity rainfalls are more likely to have differences in infiltration excess predictions with different rainfall resolutions and that a general understanding of the prevailing rainfall conditions and the soil's infiltration capacity can help in deciding whether high rainfall resolutions (below 1 h) are required for accurate surface runoff predictions.

Correspondence to: C. Hinz
(christoph.hinz@uwa.edu.au)

1 Introduction

There have been a number of studies that have suggested that including the rainfall intensities throughout a storm may affect our modelled results. Wainwright and Parsons (2002) showed that overland flow models that use mean rainfall intensity under predict surface runoff. Bronstert and Bardossy (2003) found that 1 hour resolution clearly underestimated runoff volumes attributed to Hortonian overland flow (infiltration excess). Mertens et al. (2002) compared simulated surface runoff using HYDRUS-1D and 10 min rainfall data to results using the Soil Conservation Service (SCS) runoff curve-number method and found that depending on the season or storm intensity, the curve-number method overestimates surface runoff (winter) or underestimates surface runoff (summer). Reaney et al. (2007) showed that the temporal structure of rainfall intensities within a storm event can increase or decrease the amount of runoff leaving the slope when compared to runoff predictions from constant rainfall intensities. These studies highlight the need to understand the effects of rainfall resolution on surface runoff predictions.

Published by Copernicus GmbH on behalf of the European Geosciences Union.

Whilst Bronstert and Bardossy (2003) conclude that the use of high rainfall resolution is most important for high rainfall events but not extreme events there is no clear sensitivity analysis as to the conditions where surface runoff predictions are most affected by rainfall resolution and to what extent differences in hillslope surface runoff predictions are the result of discrepancies in point scale surface runoff predictions or hillslope runoff transformations.

The earlier work of Woolhiser and Goodrich (1988) goes some way in addressing this issue with the construction of dimensionless parameters in relation to kinematic equilibria of overland flow and the ratio of the infiltration depth at ponding to the mean storm depth. This study looks at Hortonian overland flow and concentrates on the differences in peak runoff rates with the biggest differences in peak runoff rates occurring between constant rainfall and temporally varying rainfall when the ratio of the infiltration depth at ponding to the mean storm depth is low and the ratio of the time to kinematic equilibrium on the overland flow plane to the mean duration of the storm set is also low.

These previous studies into the impacts of temporally varying rainfall and surface runoff predictions have concentrated on Hortonian overland flow and do not consider differences in water able to enter the soil or surface runoff attributed to saturation excess. This study aims to expand on previous research a number of ways. Firstly, by looking at two different mechanisms of runoff generation, infiltration excess and saturation excess and how rainfall resolution may impact predictions of the mechanism dominating runoff generation. This modelling approach not only sets out to investigate differences in amounts of infiltration excess and saturation excess but also the dynamics, including maximum intensity, frequency and duration each surface runoff process is active throughout each storm event. Secondly, we quantify the effects of rainfall resolution on surface runoff generation and identify scaled rainfall and soil conditions in which model predictions are most sensitive to rainfall resolution. The scaling approach allows us to investigate a wider range of soil-storm relationships than studies based on specific conditions. An application of this approach to rainfall from a number of locations is made in an attempt to illustrate how the model can be used to gain an understanding of the sensitivity of surface runoff predictions to rainfall resolution in different rainfall regions within Western Australia.

The recognition of the importance of using high resolution rainfall data has lead to the use of stochastic simulation of rainfall and analysis of the statistical properties of hydrological modelling. For this reason, in the last 20 years there have been many studies into the transformation of available rainfall data from one scale to another (for an overview see Lovejoy and Schertzer, 2005). All disaggregation methods are based on describing the variability at one scale in relation to the variability at another scale. One of the most prevalent and promising methods is the use of multifractal random cascades which are able to reproduce the statistical properties of non-extreme rainfall events as well as extreme rainfall events (Veneziano et al., 1996, Over and Gupta, 1996, Menabde et al., 1997). In this paper we use the bounded random cascade approach described by Menabde and Sivapalan (2000) with three different sets of rainfall parameters from Western Australia as an illustration of a method to determine the soil-storm relationships most sensitive to rainfall resolution when predicting surface runoff and how this may change for different rainfall regions.

The results presented in this paper remain at the point scale. The authors wish to create a clear and accurate understanding of the processes at the point scale and how these may be influenced by different soil-storm properties before these effects are further complicated by hillslope properties such as steepness, length and roughness. "*Even at the point scale there is much that remains to be learned about how best to represent the dynamic characteristics of infiltration and surface runoff generation*" (Beven, 2002, pp. 80).

Whilst using complex rainfall as input, we used a simple infiltration capacity threshold in a similar fashion to Yu et al. (1997) to determine infiltration excess. The simple infiltration capacity threshold was chosen as Yu (1999) points out that the widely used Green-Ampt approach has been applied mostly in relation to predicting runoff amounts as opposed to runoff rates which we also wish to predict here. Yu et al. (1997) showed that at 1 min intervals infiltration rates were closely related to rainfall intensities and were "*essentially independent of cumulative infiltration amount, features not in accord with the Green-Ampt infiltration equation*" (pp. 1295). Comparison of the Green-Ampt approach to a simple infiltration capacity threshold approach showed that the simple threshold outperformed the Green-Ampt approach when compared to runoff data at a range of time intervals and storm events, as it was better able to represent runoff hydrographs and peak runoff rates (Yu, 1999). The aim of this paper is to investigate surface runoff predictions at a range of rainfall resolutions including high resolution rainfall less than 5 min and also to look at the dynamics of this predicted surface runoff. From the evidence outlined in Yu et al. (1997) and Yu (1999) we have adopted a point scale model that incorporates a single infiltration capacity.

Saturation excess is predicted using a simple, lumped parameter bucket model. There are numerous examples of the use of simple lumped storage representations of surface hydrology (Milly, 1994; Kirkby and Cox, 1995; Farmer et al., 2003; Woods, 2003; Struthers et al., 2007a, b). It is this minimalist, process based approach, as opposed to a more complicated Richards equation, that we wish to adopt in our attempts to investigate how using rainfall measured at various time scales will influence the triggering of surface runoff thresholds. Using this minimalist approach we are able to derive scaled soil-storm properties that relate a wide range of soil and storm conditions to the impact of time averaged rainfall data on surface runoff predictions. Although these point scale saturation excess predictions have limited application

as the model does not account for two and three dimensional aspects, the authors believe the inclusion of this storage element in the model is important in investigating the effects of rainfall resolution on processes which are buffered by soil storage and drainage and dependent on the differences in soil infiltration created from the interaction of the different rainfall resolutions and the infiltration capacity threshold.

This study has important implications for the accuracy of current hydrological models that use temporally averaged rainfall inputs. It offers a means by which we can predict how point scale surface runoff predictions may be influenced by the resolution of input rainfall data and under what conditions the temporal scaling of rainfall may not only affect surface runoff amounts but also the dominant runoff generating process and the dynamics of this surface runoff.

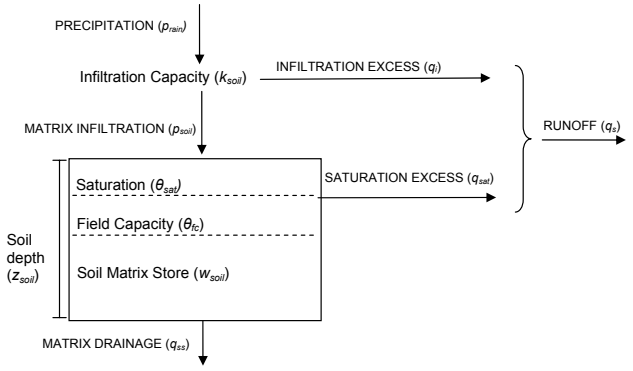

Fig. 1. Diagram of the conceptual bucket model. Fluxes are written in capitals and thresholds in lower case.

2 Methods

2.1 Conceptual model

A one dimensional, conceptual bucket model, in accord with Woods (2003), was developed that instantaneously partitions rainfall into infiltration excess q_i (mm min^{-1}), infiltration p_{soil} (mm min^{-1}), soil storage w_{soil} (mm), soil drainage q_{ss} (mm min^{-1}) and matrix saturation excess $q-$sat (mm min^{-1}). Fluxes into and out of the soil store were controlled by simple thresholds, infiltration capacity k_{soil} (mm min^{-1}), field capacity θ_{fc} (–) and matrix saturation θ_{sat} (–) (Fig. 1).

We use a very simple maximum infiltration capacity threshold controlling the amount of water entering the soil profile which is similar to the classic Horton overland flow model (Horton, 1933). The input of water to the soil profile is represented as an intensity over time $p_{\text{soil}}(t)$ (mm min^{-1}). If the rainfall intensity p_{rain} (t) (mm min^{-1}) exceeds the infiltration capacity k_{soil}, input is then equal to the infiltration capacity k_{soil}:

$$p_{\text{soil}}(t) = \begin{cases} p_{\text{rain}}(t) & \text{if } p_{\text{rain}}(t) \le k_{\text{soil}} \\ k_{\text{soil}} & \text{if } p_{\text{rain}}(t) > k_{\text{soil}} \end{cases} \quad (1)$$

The remaining water becomes infiltration excess, q_i:

$$q_i(t) = \begin{cases} 0 & \text{if } p_{\text{rain}}(t) \le k_{\text{soil}} \\ (p_{\text{rain}}(t) - k_{\text{soil}}) & \text{if } p_{\text{rain}}(t) > k_{\text{soil}} \end{cases} \quad (2)$$

To simulate an infiltration capacity that decreases with time this model can incorporate an initial, cumulative amount of infiltration (F_0) required before the infiltration capacity threshold starts taking effect (Yu et al., 1997).

Drainage, $q_{ss,}$ occurs when the soil storage reaches a critical threshold (field capacity, θ_{fc}) (Struthers et al., 2007a):

$$q_{ss}(t) = \begin{cases} 0 & \text{if } w_{\text{soil}}(t) < \theta_{\text{fc}} z_{\text{soil}} \\ (w_{\text{soil}}(t) - \theta_{\text{fc}} z_{\text{soil}})/\tau_{\text{soil}} & \text{if } w_{\text{soil}}(t) \ge \theta_{\text{fc}} z_{\text{soil}} \end{cases} \quad (3)$$

where z_{soil} is the soil depth (mm) and τ_{soil} is a drainage response time (min). Struthers et al. (2006) showed that the drainage parameters of a lumped parameter bucket model are related to the drainage recession response based on the unsaturated hydraulic conductivity function of Brooks and Corey (1964).

Matrix saturation, q_{sat}, occurs when the soil store becomes full. Water can only infiltrate as fast as the soil is draining, therefore matrix saturation excess becomes the input of water to the soil profile minus drainage:

$$q_{\text{sat}}(t) = \begin{cases} p_{\text{soil}}(t) - (\theta_{\text{sat}} - \theta_{\text{fc}}) z_{\text{soil}}/\tau_{\text{soil}} & \text{if } p_{\text{soil}}(t) > (\theta_{\text{sat}} - \theta_{\text{fc}}) z_{\text{soil}}/\tau_{\text{soil}} \text{ and } w_{\text{soil}}(t) = \theta_{\text{sat}} z_{\text{soil}} \\ 0 & \text{if } w_{\text{soil}}(t) < \theta_{\text{sat}} z_{\text{soil}} \text{ or } p_{\text{soil}}(t) \le (\theta_{\text{sat}} - \theta_{\text{fc}}) z_{\text{soil}}/\tau_{\text{soil}} \end{cases} \quad (4)$$

The authors acknowledge that saturation excess runoff is most of the time not a point scale process and is influenced by landscape properties such as topography and ground water conditions, however for simplicity we base our model on the assumptions that there is no water table interaction, the lower boundary is highly permeable and lateral subsurface water flow is negligible. As a result the saturation excess runoff at the point scale is controlled purely by soil properties. Despite these assumptions, the authors believe the inclusion of saturation excess in the model is an important illustration of how rainfall resolution influences a surface runoff generating mechanism that is buffered by soil water storage and dependent on the differences in infiltration created by the interaction between rainfall resolution and the infiltration capacity threshold.

Surface runoff, q_s (mm min^{-1}), can be generated two ways, saturation excess or infiltration excess and becomes the sum of infiltration excess q_i and matrix saturation excess q_{sat}:

$$q_s(t) = q_{\text{sat}}(t) + q_i(t) \quad (5)$$

As the model is being applied on a storm event basis it is assumed that when rain is falling no evaporation takes place.

Table 1. Soil parameters used for simulations.

	k_{soil} (mm h^{-1})	τ_{soil} (–)	z_{soil} (mm)	θ_{wp} (–)	θ_{fc} (–)	θ_{sat} (–)	f^* (–)
Clay	12	20	100	0.15	0.30	0.50	2.40
			240				1.00
			500				0.48
			900				0.27
			1200				0.20
			1300				0.18
Loam	24	2	100	0.10	0.25	0.45	0.48
			178				0.27
			240				0.20
			300				0.16
Layered soil	100	1	100	0.05	0.20	0.40	1.00
			208				0.48
			370				0.27
			500				0.20
Sand	100	0.2	100	0.05	0.20	0.40	0.20

Table 2. Storm properties and dimensionless infiltration parameters for three soils simulated.

Average rainfall intensity R_0=z_{storm}/t_{storm} (mm h^{-1})	Total storm depth z_{storm} (mm)	Layered soil k^* (–)	Loam k^* (–)	Clay k^* (–)
150.00	600	0.67		
100.00	400	1.00		
75.00	300	1.33		
66.75	267	1.50		
50.00	200	2.00		
40.00	160	2.50	0.60	0.30
36.00	144	2.78	0.67	0.33
32.00	128	3.13	0.75	0.38
24.00	96	4.17	1.00	0.50
20.00	80	5.00	1.20	0.75
16.00	64	6.25	1.50	1.00
12.00	48	8.33	2.00	1.50
8.00	32	12.50	3.00	2.00
6.00	24	16.67	4.00	3.00
4.00	16	25.00	6.00	4.00
2.00	8	50.00	12.00	6.00
1.00	4	100.00	24.00	12.00
0.50	2	200.00	48.00	24.00
0.25	1			48.00

The mass balance for soil water storage is accordingly given by:

$$\frac{dw_{soil}}{dt} = p_{soil}(t) - q_{ss}(t) - q_{sat}(t) \quad (6)$$

This is similar to Woods (2003) except that evaporation is neglected in our case. Equations 1 to 6 are solved by discretizing Eq. (6) and the resulting system of algebraic equations are solved implicitly using a dynamic programming method in Mathematica 5.2 (Wolfram Research Inc., 2005).

Simulations were run for a clay, loam, sand and layered (duplex) soil for which the parameter values are listed in Table 1. Parameters for the saturated water content θ_{sat}, field capacity θ_{fc} and wilting point θ_{wp} were taken from Rawls et al. (1992). The drainage response time, τ_{soil}, was taken as order of magnitude estimates from saturated hydraulic conductivity for a 100 mm soil depth from Rawls et al. (1992) as per Struthers et al. (2007a). The infiltration capacities k_{soil} used were 12, 24 and 100 mm h^{-1}. This provided an order of magnitude range and a range of two orders of magnitude in the dimensionless analysis presented below. The layered soil, a coarse textured soil overlaying a finer textured soil with a sharp boundary, is commonly referred to in Australia as a duplex soil and had a high infiltration capacity and a slower drainage due to this finer textured impeding layer. This was used as these soils are common in Australia and it allowed us to test the effect of changing the ratios of infiltration capacity and drainage rates. Simulations were run with initial conditions at field capacity and at wilting point.

2.2 Storm generation

Average storm properties used in the study are presented in Table 2. Total storm depth z_{storm} ranged from 1 to 600 mm. A constant storm duration, t_{storm}, of four hours was used. The mean intensities z_{storm}/t_{storm} ranged from 0.25 to 150 mm h^{-1} and were chosen to allow for a wide range of scaled parameters (to be described later in Sect. 2.4) rather than to reflect the predominant rainfall intensities in Australia. The probability of these rainfall events will be discussed later in Sect. 2.5. The storm duration was kept constant for scaling purposes but initial analysis of different durations shows the same patterns of results. Four hour storms represent the approximate average storm durations in the south-west of Australia (Hipsey et al., 2003).

Rainfall intensities at these different resolutions were generated using the bounded random cascade model (Menabde and Sivapalan, 2000) firstly parameterized to south-western Australian rainfall (Hipsey et al., 2003). Random cascades are based on the apparent multifractal scaling behaviour of rainfall. Rainfall variability at different time scales is determined by the analysis of break down coefficients, $u(\tau, i)$, which are defined as "*the ratio of rainfall of a random field averaged over different scales where the smaller is contained within the larger*" (Harris et al., 1998, pp. 93):

$$u(\tau, i) = \frac{R_\tau(t_n)}{R_i(t_n)} \quad \tau < i \tag{7}$$

where R_τ (t_n) and R_i (t_n) are the rainfall totals accumulated over the durations τ and i where τ is assumed to be completely included in the interval i (Menabde and Sivapalan, 2000). For a more detailed description of breakdown coefficients and their analysis see Harris et al. (1998). Menabde and Sivapalan (2000) explain how the breakdown coefficients for the entire rain record is separated into different time intervals and the distributions of breakdown coefficients at different timescales is described by fitting a single parameter beta distribution:

$$p_U(u) = \frac{1}{B(a)} u^{a-1}(1-u)^{a-1},$$

$$\text{where } B(a) = \int_0^1 x^{a-1}(1-x)^{a-1}dx \tag{8}$$

with the sole parameter a changing with the timescale of observation t. It has been found in a number of studies that at smaller timescales the breakdown coefficients are more similar (less variable) and breakdown coefficients at larger timescales are more variable (Menabde et al., 1997; Harris et al., 1998; Menabde and Sivapalan, 2000). Menabde and Sivapalan (2000) use the following scaling law to describe this dependence of the a parameter on the timescale, t:

$$a(t) = a_0 t^{-H} \tag{9}$$

A high or large a_0 parameter (y intercept) means that rainfall at small timescales is less variable (more constant). In contrast, a low or small a_0 parameter would indicate more variability of rainfall intensities at small time intervals. The H parameter describes the slope of this relationship and hence the rate of change of variability with increasing time intervals.

Rainfall is generated by starting with an initial homogeneous storm of a certain length (t_{storm}) and average storm intensity R_0. The next step is to divide the original storm duration (t_{storm}) into two halves and assign each half a value R_1 and R_2 where the sum of $R_1 t$ and $R_2 t$=$R_0 t$ and the weights at any level n, are drawn from the beta distribution with its sole parameter a estimated from relationship (9). See Fig. 2 for an example of storm intensities generated for three different time scales (t). For further details on the generation of rainfall see Menabde and Sivapalan (2000).

The four hour storm duration was long enough to investigate 6 cascades of rainfall resolutions (120, 60, 30, 15, 7.5, 3.75, 1.875 min) with the resolution halving at each cascade (t_n=$2^n t_0$) with n=0, 1 ,2, ... 6 and t_0=1.875 min. To ensure that rainfall input into the rainfall partitioning model was at the same resolution (1.875 min), all input vectors had a length of 128 (240/1.875). Intensities at lower resolutions were repeated (time step (t^n)/1.875) times so that all vector lengths were the same.

An initial analysis of distributions of storms generated using the model was conducted to determine a statistically stable number of storm realizations to be used in the analysis. The first, second and third moments were calculated for distributions of rainfall intensities from x realizations of a storm event (x= 25, 50, 100, 250, 500, 750, 1000, 2000). At x=500 the variations in the moments converged so that distributions with x values greater than 500 were not significantly different (T test, p=0.05) from x=500. For this reason, five hundred realizations of each storm were used in the analysis.

2.3 Output analysis

At the end of each simulation the total amount of infiltration excess, saturation excess, deep drainage and runoff were calculated (mm). The first, second and third moments of the distributions of these amounts as well as the distributions of the maximum intensities (mm min^{-1}), frequencies and durations (min) each surface runoff process was active throughout each storm event. The moments of the distributions of the scaled outputs were also calculated and used to compare the response of different soils to different storm properties.

2.4 Scaling of outputs

To determine the soil and rainfall conditions where model predictions of infiltration excess and saturation excess were most sensitive to rainfall resolution for a wider range of parameters we scaled our model outputs and soil properties with average storm intensities. All model output intensities were multiplied by the time step and divided by the storm

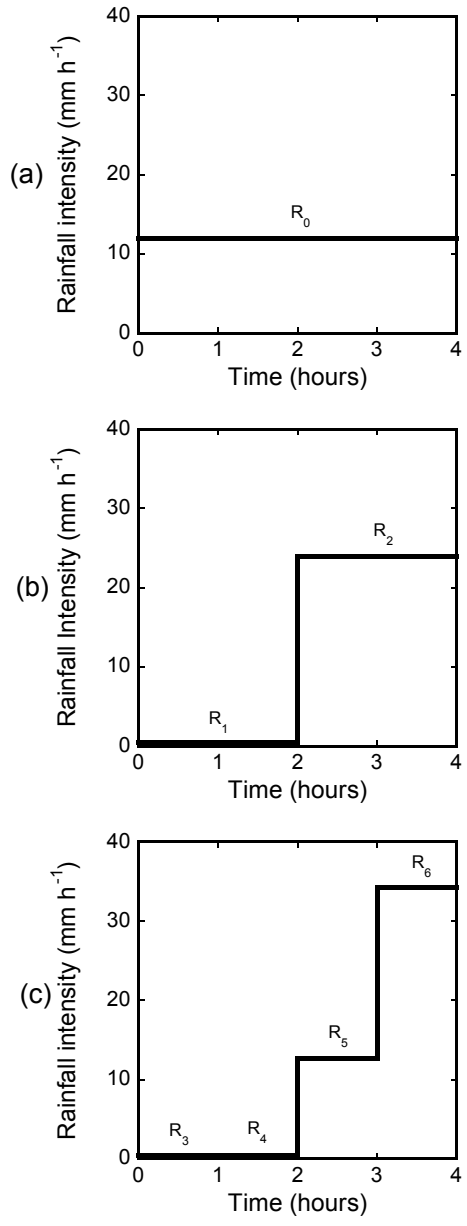

Fig. 2. Diagram of rainfall generation at cascading time steps (4 h, 2 h and 1 h).

depth making them dimensionless. These dimensionless outputs were related to three dimensionless scaling parameters that were derived from three groups of dimensional parameters that characterise the soil and the averaged rainfall properties. The soil parameters were the infiltration capacity k_{soil} (Eq. 1) and the ratio of soil depth and drainage response time $z_{\text{soil}}/\tau_{\text{soil}}$ (Eq. 3) controlling the drainage behaviour. From here on this ratio ($z_{\text{soil}}/\tau_{\text{soil}}$) will be referred to as the drainage coefficient. The average rainfall was fully characterized by the average intensity $z_{\text{storm}}/t_{\text{storm}}$. All groups were rates in mm min^{-1} and ratios of these groups were used to carry out the scaling analysis presented below.

Infiltration excess was produced when the supply of water (rainfall) exceeded the soil infiltration capacity threshold. By relating these two properties we could determine the amount of dimensionless infiltration excess for a range of infiltration capacities and average storm intensities using one curve. The scaling parameter we used to do this was k^* (–) which is the ratio of maximum soil infiltration capacity to the average storm intensity:

$$k^* = \frac{k_{\text{soil}} t_{\text{storm}}}{z_{\text{storm}}} \tag{10}$$

The range of k^* values was 0.3 to 200 (Table 2). The higher the average storm intensity relative to the infiltration capacity is, the smaller the k^* value.

Saturation excess occurred when the difference between the flux of water entering the soil and the flux of water leaving the soil (drainage) exceeded the soil storage capacity. The second dimensionless parameter, f^* (–), relates soil properties controlling the input of water (infiltration capacity, k_{soil}) to the drainage coefficient ($z_{\text{soil}}/\tau_{\text{soil}}$) which represents the soil properties controlling the output of water:

$$f^* = \frac{k_{\text{soil}} \tau_{\text{soil}}}{z_{\text{soil}}} \tag{11}$$

The higher the infiltration rate multiplied by the drainage rate the deeper the soil required to maintain the same f^* value. The range of f^* values is presented in Table 1. The range of f^* parameters was limited to soil depths no shallower than 100 mm. For the sand, with a high infiltration capacity and fast drainage rate even at the shallowest soil depth (100 mm) no saturation excess was produced, making this the only depth simulated.

Now the soil properties that control saturation excess have been scaled (using f^*) we need to relate them to the storm properties that produce saturation excess. By doing this we could determine the storm properties at which saturation excess was most sensitive to rainfall resolution for our range of f^* parameters. This was done by constructing the g^* parameter which is the average storm intensity in relation to the drainage coefficient:

$$g^* = \frac{t_{\text{storm}} z_{\text{soil}}}{z_{\text{storm}} \tau_{\text{soil}}} = \frac{k^*}{f^*} \tag{12}$$

2.5 Application to different rainfall regions

To investigate the influence of rainfall generated from different rainfall regions we concentrated on infiltration excess predictions as we have already discussed the limitations of applying the saturation excess predictions. We began by looking at how the within storm temporal variability influences the soil-storm scaling relationship outlined above. We then looked at the average storm intensities of different locations and the fraction of storms for each location likely to affect infiltration excess predictions if low resolution rainfall is used.

Table 3. Rainfall data and bounded random cascade parameters for locations in different rainfall regions in Western Australia.

Location	Latitude	Longitude	Years of one minute data	a_0	H
Newdegate	−32.02	116.52	22	15.0	−0.47
Kalgoorlie	−30.78	121.45	3	10.8	−0.44
Port Hedland	−20.37	118.63	3	5.8	−0.35
Broome	−17.95	122.23	3		
Perth	−31.95	115.87	3		

To investigate the effect of different within storm patterns from different rainfall regions rainfall was generated using a_0 and H parameters fitted to rainfall from three locations in Western Australia. These locations included Newdegate, Kalgoorlie and Port Hedland. The parameterization of the bounded random cascade model to 15 different locations in Western Australia found that Newdegate had the least within storm variability, Port Hedland had the most variable within storm patterns and Kalgoorlie was in between (Hearman and Hinz, 2007[1]). See Table 3 for these parameters. Newdegate is located in the south west, the same location as Hipsey et al. (2003) and experiences predominantly winter rainfall (June to August) in the form of advective fronts. Port Hedland and Kalgoorlie are located in arid regions of the state. Port Hedland is in the tropics and receives convective and cyclonic rain predominantly in the summer months. Kalgoorlie is located further south and inland and has less intense and less seasonal rainfall. The same point scale rainfall partitioning model and soil-storm scaling (as outlined above) was applied to rainfall generated from these three locations and the effect of different within storm variability on the differences in point scale infiltration excess predictions using different rainfall resolutions was determined.

An investigation of the effect of locations in different rainfall regions on the likelihood infiltration excess predictions will be affected by rainfall resolution was done using one minute rainfall data from five locations in Western Australia. These locations included the three outlined above, as well as Broome, located in the north east of Western Australia and experiencing summer monsoonal rain, and Perth, located on the coast of the south west region. This was done by calculating average storm intensities from the one minute rainfall where a storm was identified as having 7 h between rainfall measurements. Then, using the average storm intensities, k^* values were calculated for clay, loam and sandy soils. From the results of the scaling of differences in infiltration excess predictions using different rainfall resolutions we were able to identify the fraction of storms where rainfall resolution was likely to affect infiltration excess predictions using the calculated k^* values for each soil from each location.

[1]Hearman, A. J. and Hinz, C.: Within storm rainfall variability in Western Australia, in preparation, 2007.

3 Results and discussion

3.1 Model output

The rainfall resolution influenced the amount and dynamics of infiltration excess and saturation excess runoff predictions. Figure 3 is an example of the model output for a single storm event showing two different rainfall resolutions; 1.875 min (black line) and 120 min (broken line). From this figure it can be seen that the higher resolution rainfall had higher peaks in intensities than the low resolution rainfall. This lead to infiltration excess being triggered when high resolution rainfall was used and not when the low resolution rainfall was used. As a result more water was able to enter the soil for the low resolution rainfall and the soil was saturated for a longer period of time.

Figure 3 demonstrates that not only were the processes that generated runoff different for the two different rainfall resolutions but also the dynamics of runoff produced from the different rainfall resolutions. High resolution rainfall generated more runoff with higher peaks in intensity. From this example we illustrate that rainfall resolution has a direct impact on the triggering of thresholds, in particular, infiltration excess. Models using time averaged rainfall would need to calibrate this threshold to a lower effective k_{soil} if they are to fit their model predictions to field measurements. However, even if the model is able to be calibrated to give the correct infiltration excess amount, using low resolution rainfall will give different dynamics. Low resolution rainfall will lead to long, low intensity predictions of runoff, whereas high resolution rainfall will lead to short, more intense bursts of runoff. The implications of these different surface runoff dynamics will be discussed later in the dynamics Sect. 3.5.

Whilst Fig. 3 is an example of one storm realization, the results presented in the sections that follow consider the statistical properties of the response, in particular the means of the distributions produced from 500 of these realizations and how these relate to scaled soil-storm properties.

3.2 Infiltration excess

Using low rainfall resolution under predicted infiltration excess. This under prediction of infiltration excess can be seen in Fig. 4a where the high resolution rainfall of 1.875 min

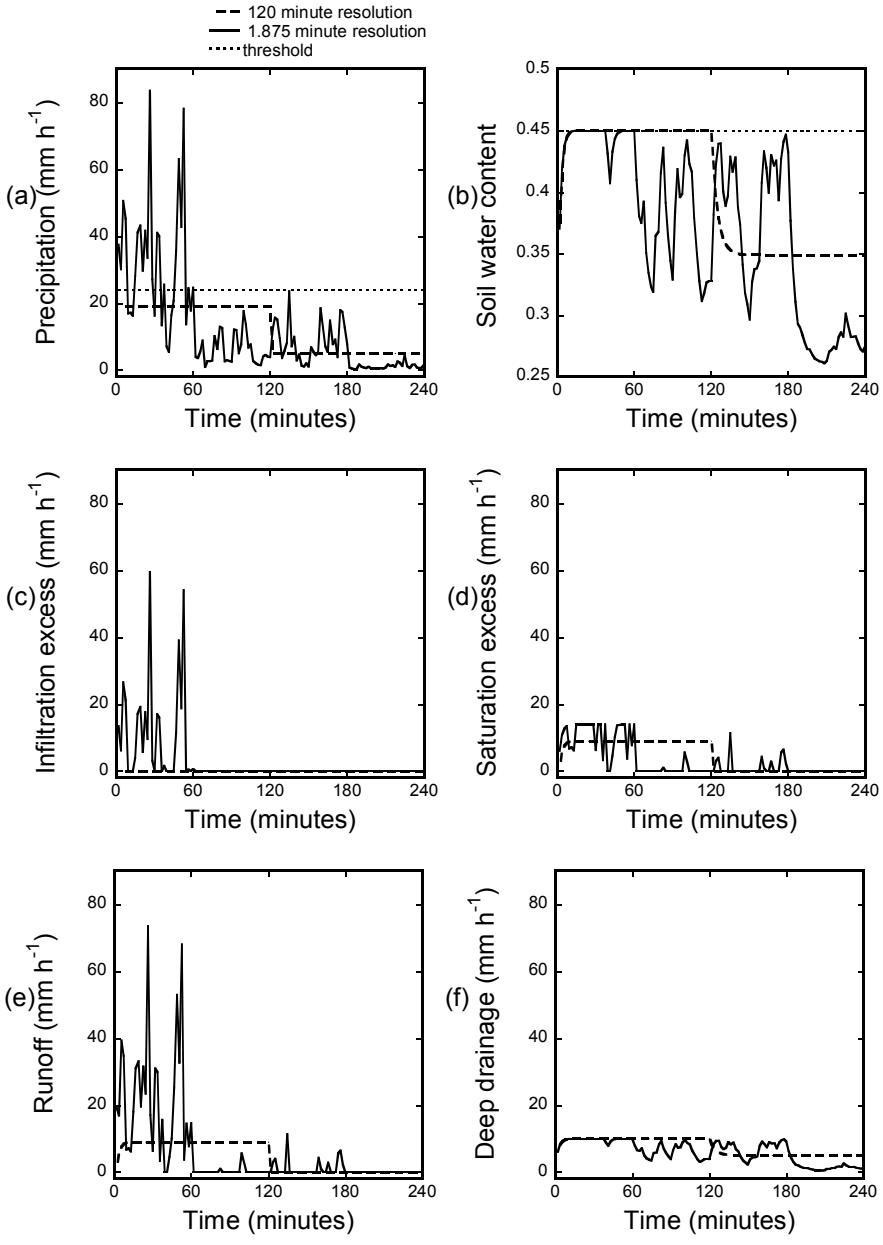

Fig. 3. Example of the model input (precipitation **(a)**) and model outputs (soil water content **(b)**, infiltration excess **(c)**, saturation excess **(d)**, runoff **(e)** and deep drainage **(f)**). Produced from one storm (48 mm) at two different rainfall resolutions (1.875 min and 120 min) for a loam soil with a depth of 100 mm.

(n=0) produced more infiltration excess than the low resolution rainfall of 120 min (n=6). This figure also demonstrates that for different k^* values, the slopes of these curves, or the sensitivity to rainfall resolution were different. The sensitivity of predicted amounts of infiltration excess was summarized in Fig. 4b which shows the differences in infiltration amounts between 1.875 min resolution and 120 min resolution, which is the first point minus the last point for each curve in Fig. 4a. It can be seen that the scaling allows the curves for all soil types to collapse. They were most sensitive to rainfall resolution when the soil infiltration rate was 1.5 times the average storm intensity ($\ln k^*$=0.4), and at this point the amount of infiltration excess was under predicted by 26% of the total storm amount. This supports Bronstert and Bardossy (2003) who also found that the sensitivity of predictions of infiltration excess to rainfall resolution were highest where the average rainfall intensity was in the same order of magnitude as the infiltration capacity of the soil.

Analysis of differences between smaller time steps (than our maximum 120 min) and our smallest time step (1.875 min) show that the biggest differences also occur at $\ln k^*$=0.4. Using 15 min resolution (n=3) still under predicted infiltration excess by 20% and 3.75 min resolution (n=1) under predicted infiltration excess by 10% of the total storm volume at $\ln k^*$=0.4. This implies that at the point scale when the soil infiltration rate is near 1.5 times the average storm intensity the rainfall resolution will impact runoff predictions even at resolutions less than 5 min. These results contradict Bronstert and Bardossy (2003) who found that between 5 min and 1 min there was no significant difference in surface runoff predictions. This may be the result of runoff transformation processes down the hillslope as our analysis is conducted at the point scale and Bronstert and Bardossy's (2003) at the hillslope scale or a result of having an infiltration rate that changes with time. When an initial infiltration amount F_0 was introduced before the soil infiltration capacity started taking effect, the maximum difference for infiltration excess predictions using different rainfall resolutions remained at $\ln k^*$=0.4 but the size of the differences decreased with increasing F_0. Also for surface runoff predictions at larger scales not only is the interaction of infiltration properties and storms important but also hillslope properties that control runoff response times (Woolhiser and Goodrich, 1988).

The sensitivity of point scale infiltration excess predictions to rainfall resolutions can be explained by the way the different rainfall resolutions triggered the infiltration excess threshold. At $\ln k^*$ values greater than 1.5, neither the high resolution rainfall nor the low resolution rainfall intensities were high enough to trigger infiltration excess. Where $\ln k^*$ was between 1.5 and 0.4, increasing the intensity of the storm lead to an increase in the amount of infiltration excess triggered by the high resolution rainfall, whereas the low resolution rainfall intensities were not high enough to trigger this threshold. Where $\ln k^*$ was less than 0.4, the dimensionless difference in infiltration excess amounts decreased. This was because at $\ln k^*$=0.4, infiltration excess was first triggered in the low resolution rainfall. The amount of infiltration excess then increased more rapidly for the low resolution rainfall than for the high resolution rainfall. This was because the low resolution rainfall had longer time steps so once these intensities began to trigger the threshold they spent a longer period of time above the threshold. At $\ln k^*$=0.4, where the maximum difference between the two resolutions occurred, the low resolution rainfall first triggered the infiltration excess threshold and therefore became the point where the biggest difference between the amounts of infiltration excess produced from the different rainfall resolutions occurred (see Fig. 7e(i), 7f(i)).

These results highlight how point scale infiltration excess predictions can be influenced by rainfall resolution and the sensitivity of these predictions to rainfall resolution depends on the relationship between rainfall intensities and soil infiltration properties. The advantage of scaling our results is that this sensitivity curve can be used to describe the sensitivity of different locations with different soil types and predominant rainfall properties. We look specifically at different rainfall regions later in Sect. 3.6. Although this analysis looks at different soil textures and does not specifically address different soil structures and macropores, if the infiltration capacity of different soil structures or macropores can be predicted then they can be incorporated into the sensitivity curve by adjusting the infiltration capacity. Struthers et al. (2007b) showed that with a similar focus on soil and storm properties the fraction of storms that trigger macropore flow could be estimated from average storm and soil properties and did not require simulations. Considering infiltration excess is a dominant surface runoff generating mechanism in Australia (Potter et

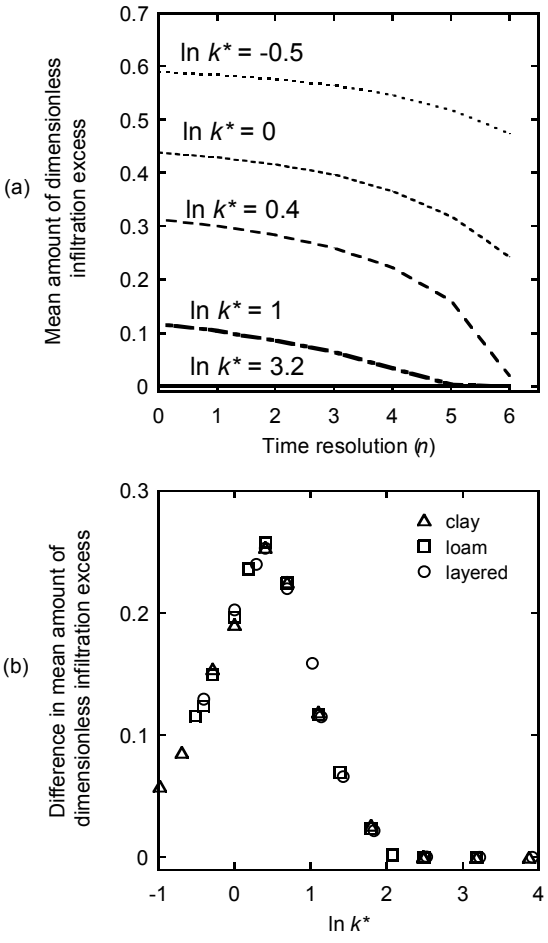

Fig. 4. The changes in mean amount of dimensionless infiltration excess with the 7 different time resolutions tested (n=0,1,2...6, t_n=2^n t_0 where t_0=1.875 min) for a loam soil at various mean rainfall intensities relative to the infiltration capacity, k^* **(a)** and the difference in mean dimensionless amount of infiltration excess between 1.875 and 120 min resolution according to changes in the natural log of k^* for the clay, loam and layered soils **(b)**.

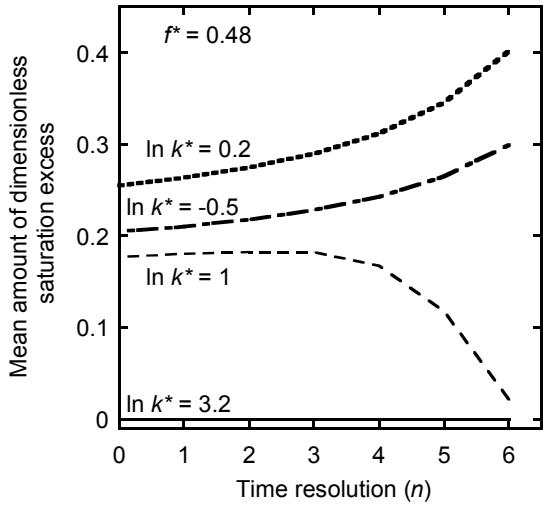

Fig. 5. The changes in mean amount of dimensionless saturation excess with the natural log of the 6 different time resolutions tested (n=0,1,2...6, t_n=2^n t_0 where t_0=1.875 min for a loam soil with an initial water content at field capacity for storms with different mean rainfall intensities relative to the infiltration capacity (k^*).

al., 2005) this simple method could prove useful in gaining an understanding of whether high resolution rainfall data is required to accurately predict surface runoff for a particular location.

3.3 Saturation excess

Whilst the saturation excess predictions cannot be applied in such a direct way as the infiltration excess sensitivity curve due to larger scale processes which are not considered here, the authors believe the saturation excess results illustrate how rainfall resolution can influence a surface runoff generating mechanism that is buffered by soil water storage and dependent on the differences in soil infiltration created from the interaction of the different rainfall resolutions and the infiltration capacity threshold.

Many surface runoff models do not attempt to model both surface runoff generating mechanisms (infiltration excess and saturation excess) and instead assume one or the other. Whilst previous studies of Australian surface runoff indicate that infiltration excess or Hortonian overland flow is the predominant mechanism, in other climates and regions of the world (more humid) surface runoff can be dominated by saturation excess or change between saturation excess and infiltration excess seasonally. Our results indicate that under certain soil-storm properties rainfall resolution may influence what process may dominate predicted surface runoff generation.

Our simulations indicated that for soils with a drainage coefficient greater than 5 times the infiltration capacity, $f^* \leq 0.2$, no saturation excess was triggered by either rainfall resolution. These findings enabled us to split our soil into two groups, those susceptible to saturation excess with f^* values greater than 0.2 (which will be presented in this section) and those not susceptible to saturation excess with f^* values equal or less than 0.2. That is, fast draining and/or deep soils were not likely to produce saturation excess unless influenced by a rising water table or topographic features (not considered here). This means for the fast draining sand tested, with f^*=0.2, even at a shallow soil depth of 100 mm no saturation excess was produced from either rainfall resolution (assuming the lower boundary is highly permeable). The effect of having a less permeable lower boundary was investigated by using a layered soil with a high infiltration capacity (the same as the sand) but a slower drainage response time. Unless stipulated, the following results show simulations where the initial soil water content was at field capacity.

Using low resolution rainfall in soils with f^* values greater than 0.2 resulted in either an over prediction or an under prediction of saturation excess depending on the soil-storm relationships. Figure 5 shows how the amount of predicted saturation excess changed with different rainfall resolutions (x-axis) and with different storm intensities (various k^* values). The figure illustrates that for high rainfall intensities (low k^* values) a low resolution rainfall predicted more saturation excess than at high resolutions. As we decreased the average intensity of the storm (increase the k^* value) this difference became smaller to a point where the high resolution rainfall predicted more saturation excess than the low resolution rainfall.

These differences in predictions of saturation excess using 1.875 min rainfall and 120 min rainfall (i.e. the mean amount predicted using 1.875 min rainfall minus the mean amount predicted using 120 min rainfall) for different soil types and soil depths are shown in Fig. 6. From this graph it can be seen that the maximum difference in over predictions of saturation excess (where the differences are most negative) scale with k^* and occur at $\ln k^*$=0.4. This is because this is the point where there is the biggest difference in predictions of infiltration excess and therefore the biggest difference in amount of water entering the soil. The low resolution rainfall had no infiltration excess at this point so more water was able to enter the soil and this combined with the constant rainfall intensity lead to a greater prediction of saturation excess than that predicted using the high resolution rainfall. This highlights the interaction of the two different thresholds (infiltration capacity and soil storage capacity) and how the input resolution can control which process dominates surface runoff.

These results also highlight the differences in water able to enter the soil depending on the rainfall resolution. Our results show that for high average intensity storms using low resolution rainfall over predicts the amount of water entering the soil and may result in an over prediction of processes affected by soil water storage such as drainage and subsurface flow predictions, the leaching of agri-chemicals and our

understanding of the ecology of plant species and their adaptation to certain soil-water conditions.

The size of the over prediction of saturation excess with low rainfall resolution depended on the ratio of infiltration capacity to drainage coefficient, f^*, with higher f^* values (shallower soils relative to the infiltration capacity and drainage coefficient) resulting in bigger differences in predictions (more negative) of saturation excess. This was because less water was required to saturate the soil profile so more saturation excess was predicted from the same amount of water entering the soil profile and thus resulted in bigger differences in predictions from different rainfall resolutions.

From Fig. 6a it can be seen that the maxima of the positive differences did not all occur at the same $\ln k^*$ value. This was because infiltration excess was not being triggered at such low intensity storms. Instead, the maximum differences depended on how fast the soil was draining in relation to how fast the water was entering the soil i.e. the g^* parameter. Figure 6b presents the differences in amounts of saturation excess according to changing g^* values. It can be seen that the maxima of the positive differences in saturation excess occur when the saturated drainage rate was 7.4 times the average storm intensity ($\ln g^*$=2). This was the point where low resolution rainfall began to trigger the storage capacity threshold. These results show that in soils susceptible to saturation excess, surface runoff predictions can be affected by rainfall resolutions at lower intensity storms than soils not susceptible to saturation excess. It also demonstrates that at lower average intensity storms the rate at which water enters the soil may be under predicted with the use of low resolution rainfall and therefore result in an under prediction of drainage and the potential for the leaching of agri-chemicals.

In Fig. 6 it can be seen that the size of the negative differences clearly relate to the f^* values, but the positive differences are more variable. This can be explained by the scaling methods used. The scaling related steady state conditions or the average storm intensity to soil properties, but it did not account for the variations in intensities throughout a storm when smaller time steps were used (higher resolution rainfall). The soil storage capacity was scaled relative to steady state infiltration and drainage rates and did not account for the variations in the rate of water entering the soil when high rainfall resolutions were used. When the rainfall intensity exceeded the infiltration capacity the water entered the soil at a constant intensity (equal to the infiltration capacity) and this is why the negative differences in saturation excess scale with the f^* parameter. However, when the rainfall intensity did not exceed the soil infiltration capacity and the input was high resolution rainfall the water entered the soil at variable intensities. But the scaling did not account for the range in the rates that water could enter the soil. For this reason, differences in amounts of saturation excess between high resolution rainfall and steady state conditions were different for the soil types simulated even though these soils have the same f^* and g^* scaling parameters. For example, the clay soil, with a much slower drainage response time (τ_{soil}) required a deeper soil (5 times) to have the same drainage coefficient in relation to maximum infiltration rate than the loam soil. But the range of intensities entering the clay soil was only 0–12 mm h^{-1} in comparison to 0–24 mm h^{-1} of the loam. Meaning that the clay soil requires a higher average intensity storm relative to the drainage coefficient (smaller g^* value) before the storage capacity threshold is exceeded.

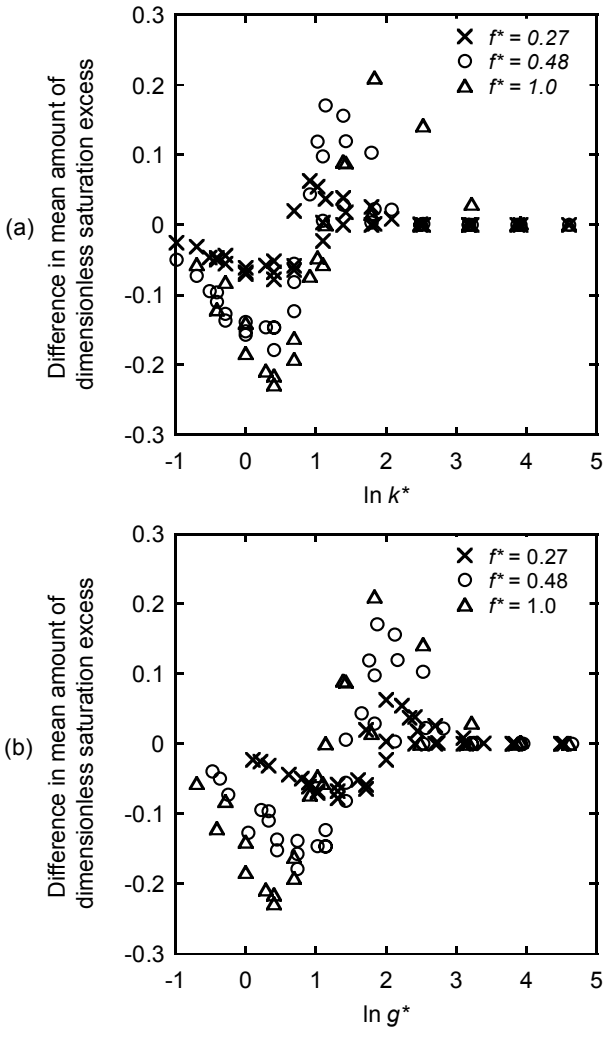

Fig. 6. The difference in mean dimensionless amount of saturation excess between 1.875 and 120 min resolution according to changes in **(a)** the natural log of k^* and **(b)** the natural log of g^* for the clay, loam and layered soils with f^* values of 0.27, 0.48 and 1 and initial soil water contents at field capacity.

An illustration of how using low resolution rainfall can change from an over prediction of saturation excess to an under prediction of saturation excess is shown in Fig. 7. This figure illustrates examples of different storms and different "stages" of threshold triggering and how this threshold

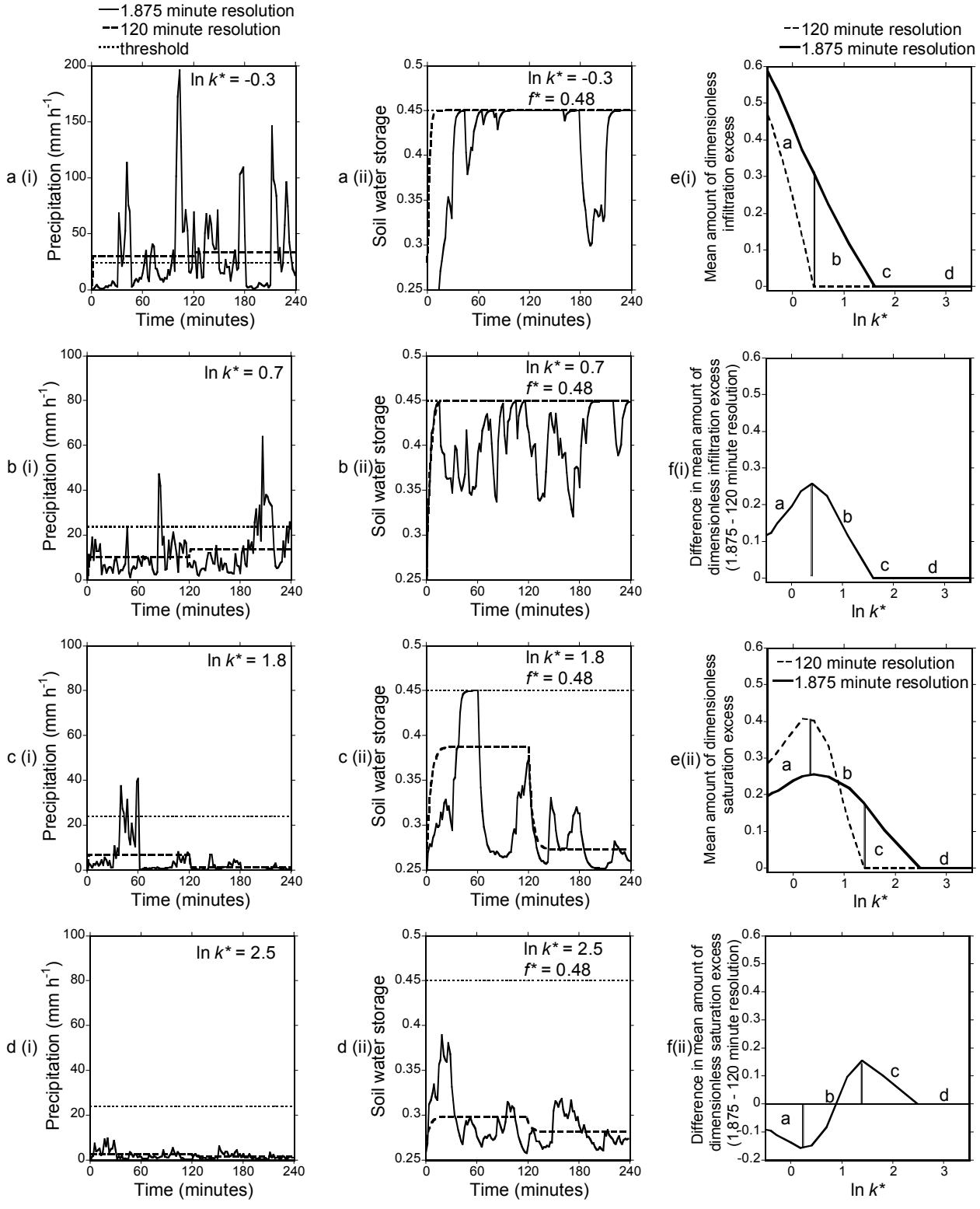

Fig. 7. An illustration of the different "stages" of threshold triggering; both resolutions trigger the thresholds (**a(i)** and **a(ii)**), only the high resolution triggers the infiltration excess threshold **(b(i))** and both resolutions trigger the storage threshold **(b(ii))**, only the high resolution rainfall triggers the saturation excess threshold **(c(ii))** and neither resolution triggers either of the thresholds (**d(i)** and **d(ii)**) and how these different "stages" relate to total storm infiltration excess **(e(i))** and saturation excess **(e(ii))** for two different resolutions and the differences in these predictions (**f(i)** and **f(ii)**) for the two resolutions.

triggering also interacts with changes in the triggering of infiltration excess.

While the initial soil moisture made a difference to the amount of surface runoff predicted it only made a small difference to the differences in predicted amounts of saturation excess between high and low resolution rainfall.

3.4 Surface runoff

Total surface runoff was a combination of infiltration excess and saturation excess and was always under predicted by low resolution rainfall (Fig. 8). The biggest differences in surface runoff occurred on soils where maximum infiltration capacities were equal to or less than 1/5th of the drainage coefficient ($f^*\leq 0.2$), when no saturation excess was produced so all surface runoff was attributed to infiltration excess. When f^* was greater than 0.2, saturation excess started to be produced and surface runoff became more sensitive to rainfall resolutions at lower intensity storms. Surface runoff predictions were most sensitive to rainfall resolution when the drainage coefficient was 7.4 times greater than average rainfall intensity ($\ln g^*=2$). The biggest differences in total surface runoff were the same as the biggest positive differences in saturation excess. This was because at this point low resolution rainfall was not producing any surface runoff and high resolution rainfall was producing saturation excess runoff. At higher rainfall intensities (lower g^*), the difference in total surface runoff amounts was smaller, but this was because the low resolution rainfall was predicting saturation excess runoff, in contrast to the high resolution rainfall which was predicting more infiltration excess. So although the sensitivity of total amounts of surface runoff appears to be lower at high intensity storms (lower g^*), the process that dominated runoff depended on the rainfall resolution. This will not only affect the dynamics of predicted surface runoff but also predicted amounts of water entering the soil and therefore predictions of soil moisture and drainage (as discussed in the saturation excess section). This is strictly valid where two and three dimensional processes such as lateral subsurface flow and groundwater interaction are negligible. This may be the case on the upper parts of a hillslope where there is no lateral flow of water.

Figure 8 has been presented according to soil types. At $f^*=0.2$, where all surface runoff was attributed to infiltration excess, the differences in predictions for all soil types were the same. For f^* values greater than 0.2 the slower draining clay soil had smaller differences than the faster draining loam and layered soils for reasons outlined in the saturation excess section. Thus, predictions of surface runoff, for all soils, were most sensitive to rainfall resolutions when all runoff was attributed to infiltration excess only.

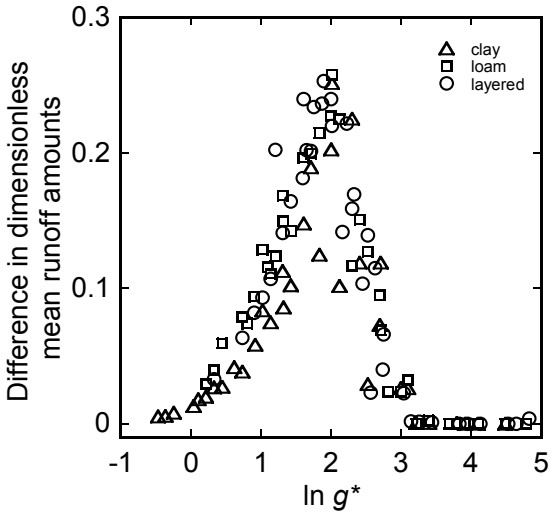

Fig. 8. The difference in dimensionless surface runoff between 1.875 and 120 min resolution according to the natural log of g^* for f^* values of 0.20, 0.27 and 0.48 for clay, loam and layered soils.

3.5 Dynamics

Not only were predicted amounts of surface runoff different according to rainfall resolution but also the dynamics of this runoff. With the high resolution rainfall having much higher intensity peaks than the lower resolution rainfall, the maximum intensities of the infiltration excess produced by the high resolution rainfall were also much higher. Maximum intensities of saturation excess produced by high resolution rainfall were buffered by an infiltration capacity and also soil depth and drainage rates. Comparing Fig. 9a(i) to 9a(ii) it can be seen that the differences in maximum saturation excess were much smaller than the differences in maximum infiltration excess. This means that when runoff was dominated by saturation excess, rainfall resolution had less effect on maximum intensities than when runoff was dominated by infiltration excess. In contrast, the differences in frequency infiltration excess and saturation excess were triggered and the differences in time both infiltration excess and saturation excess was active between resolutions was far more similar for the two different runoff processes. Surface runoff predicted by high resolution rainfall and dominated by infiltration excess had shorter more intense bursts of runoff, whereas runoff predicted by high resolution rainfall and dominated by saturation excess was more sporadic and only slightly more intense than surface runoff predicted by low resolution rainfall. To quantify this we can look at plots of the way the mean maximum intensities, the frequency and the time each process was active throughout a storm event changed with our scaling parameters, k^* and g^* (Fig. 9).

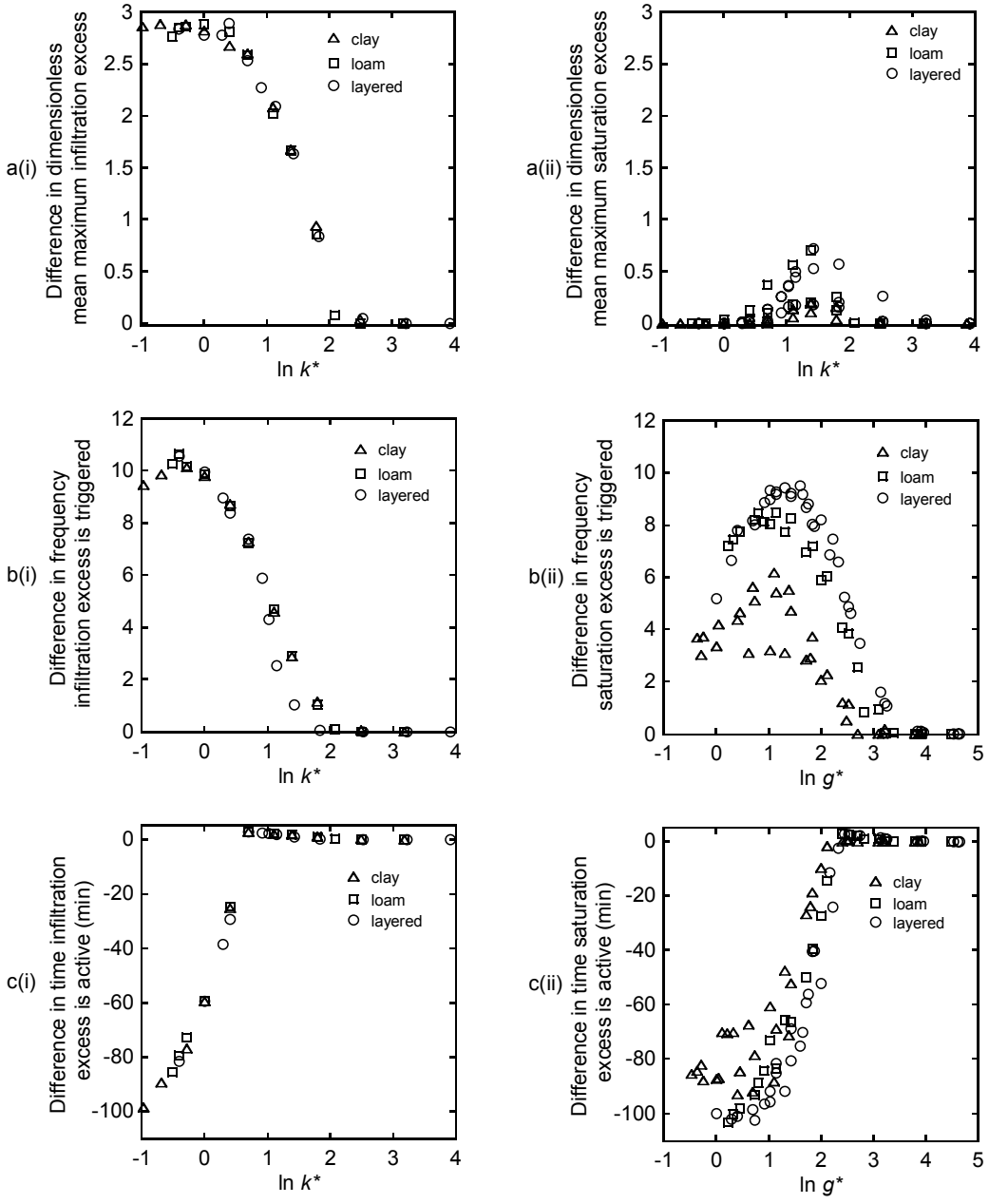

Fig. 9. Differences in the dynamics of infiltration excess (i) and saturation excess (ii) for clay, loam and layered soils with changing soil-storm properties ($\ln k^*$ and $\ln g^*$). These dynamics include dimensionless mean maximum intensities **(a)**, frequencies the threshold was triggered **(b)** and time the process was active during the storm **(c)**.

3.6 Implications for larger scale predictions

The implication of these findings to larger scales, such as the hillslope, is uncertain. Whilst our point scale results support the hillslope results of Bronstert and Bardossy (2003) who also found that the sensitivity of predictions of infiltration excess to rainfall resolution were highest when the average rainfall intensity was in the same order of magnitude as the infiltration capacity, previous studies on the effects of rainfall resolution on hillslope runoff predictions have had mixed results. Numerous larger scale (hillslope to catchment) studies have concluded that temporally averaging rainfall inputs resulted in under predictions of runoff amounts and peak runoff intensities (Bronstert and Bardossy, 2003; Wainwright and Parsons, 2002; Singh, 1997; Woolhiser and Goodrich, 1988). In constrast, Reaney et al. (2007) showed that the temporal

averaging of rainfall inputs can result in either an over prediction or an under prediction of hillslope surface runoff. Experimental studies have shown the importance of temporal rainfall structure on hillslope runoff lengths (Stomph et al., 2002; Puigdefrabregas, 1999). Puigdefabregas (1999) explains that pauses in rainfall allow overland flows to infiltrate and thus constrains overland flow lengths. In contrast, long lasting saturation excess overland flow covers greater distances (Puigdefabregas, 1999). Cameraat (2004) illustrated that the frequency of rainfall events that trigger plot scale runoff was higher than the frequency of rainfall events that trigger hillslope or catchment runoff, illustrating that at the finest scales, soil properties such as infiltration capacity are very important in controlling runoff triggering, whereas at larger scales, such as the plot and hillslope, the spatial pattern of vegetation plays an important role in the triggering of runoff thresholds. These experimental studies highlight the complex nature of scaling point scale runoff predictions to larger scale runoff predictions which is beyond the scope of this paper.

3.7 Application to other rainfall regions

When the same sensitivity analysis was applied using different rainfall parameters (more variable rainfall from the tropics) the maximum differences between runoff predicted from high and low resolution rainfall occurred at the same soil-storm properties. That is, maximum differences in infiltration excess occurred at $\ln k^*$=0.4. However with more variable rainfall these maximum differences were larger. Port Hedland, with the most variable rainfall analysed, had differences in infiltration excess predictions between 1.875 min and 120 min rainfall resolutions of 34% as compared to 26% using south west rainfall parameters (Newdegate). This illustrates that for all rainfall types this peak sensitivity of point scale surface runoff predictions to rainfall resolutions occurs at the same soil-storm relationships and can be used to predict whether rainfall resolution will influence runoff predictions for locations in different rainfall regions.

We looked at the likelihood runoff predictions will be influenced by rainfall resolution by analysing the storm properties from 5 locations across Western Australia. The average storm intensities from at least 3 years of one minute rainfall data were used to categorize the fraction of rainfall events that fall into the different categories of threshold triggering i.e. whether both resolutions trigger the infiltration excess threshold, when only the high resolution rainfall triggers the infiltration excess threshold or neither resolution triggers the infiltration excess threshold. Figure 11 illustrates the fraction of storm events that fall into these three different categories for 5 locations across Western Australia for a clay, loam and sandy soil. It can be seen that the fraction of storms which rainfall resolution may influence runoff predictions changes for different locations and soil types. The model suggests that point scale surface runoff predictions on clay soils would

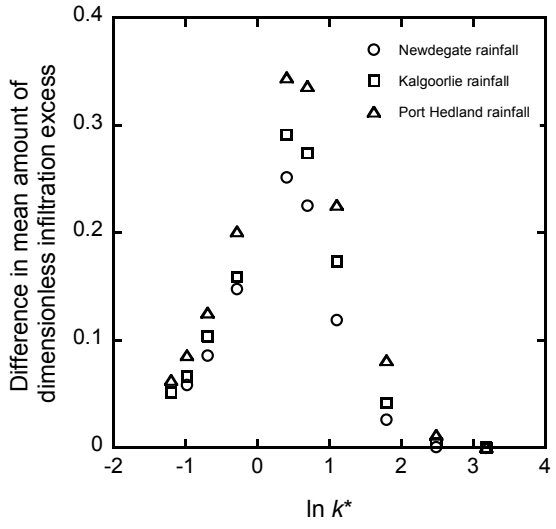

Fig. 10. Difference in the mean dimensionless amount of infiltration excess between 1.875 and 120 min resolution with changes in the natural log of k^* for rainfall generated from Newdegate, Kalgoorlie and Port Hedland.

be influenced by rainfall resolution for over 75% of rainfall events in the last 3 years in Broome and Port Hedland, located in the tropics, for 65% of events in Kalgoorlie and over 40% of events in Perth and Newdegate. For the loam soil, percentages of events in which point scale surface runoff predictions influenced by rainfall resolution ranged from 60% in Broome to 25% in Newdegate. For sandy soils with a high infiltration capacity infiltration excess predictions were only affected in rainfall regions with high intensity storms such as Broome and Port Hedland. Only 2% of rainfall events in rainfall regions with less intense rainfall events, Perth and Newdegate, caused discrepancies in infiltration excess predictions with the use of low resolution rainfall. This analysis shows that the proportion of rainfall events likely to show discrepancies in infiltration excess runoff due to different rainfall resolutions will be highest in tropical regions with high intensity storms on slow infiltrating soils and least in rainfall regions with less intense rainfall and faster infiltrating soils. A general understanding of the prevailing rainfall conditions and soil infiltration rates could prove very useful in determining whether high resolution rainfall data is required for surface runoff predictions.

4 Conclusions

This paper demonstrates that rainfall resolution has a direct effect on the triggering of point scale hydrological thresholds. It used a dimensionless analysis to highlight the soil and storm conditions where point scale surface runoff predictions were most sensitive to temporal rainfall averaging. The biggest differences in surface runoff predictions using

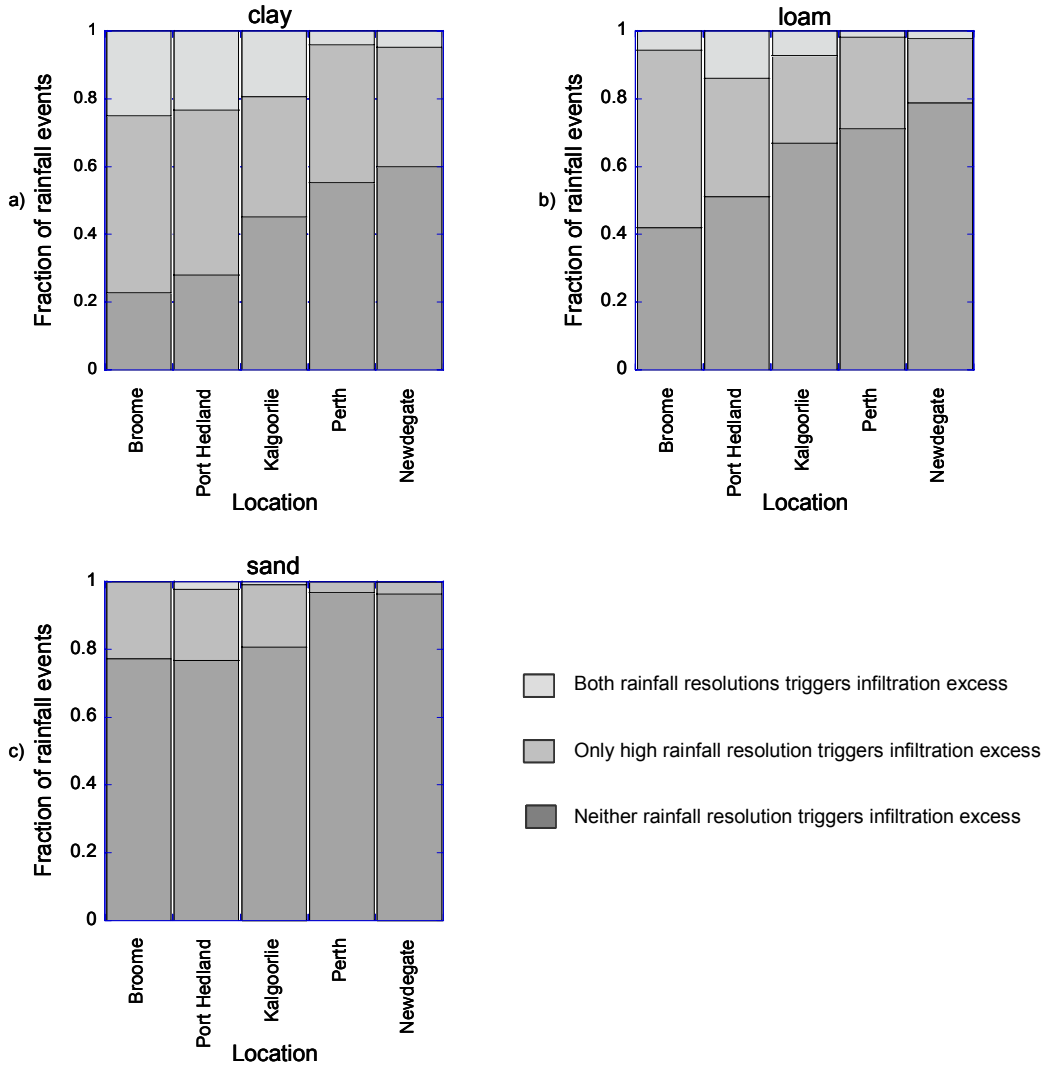

Fig. 11. The fraction of rainfall events where both rainfall resolutions trigger infiltration excess, only high resolution rainfall triggers infiltration excess or neither resolution triggers infiltration excess for a clay, loam and sand soil at different locations in Western Australia.

different rainfall resolutions occurred where surface runoff was dominated by infiltration excess and the infiltration capacity was 1.5 times the average storm intensity ($\ln k^*$=0.4). When within storm parameters from 3 different locations were used this maximum difference occurred at the same point and ranged from 26–34%. The application of this sensitivity analysis to different rainfall regions in Western Australia showed that locations with higher average storm intensities are more likely to produce differences in infiltration excess predictions with different rainfall resolutions. The study shows that a general understanding of the prevailing rainfall conditions and the soil's infiltration properties are the key to understanding whether high rainfall resolution is required for accurate point scale surface runoff predictions.

Our results question the accuracy of current hydrological models that run under the soil-storm conditions shown to be sensitive to rainfall resolution. Models operating under these conditions and using temporally averaged rainfall may need to calibrate their infiltration rate to a lower effective rate in order to fit field runoff measurements. The use of low resolution rainfall may over predict the amount of water entering the soil and therefore soil water content and drainage at high intensity storms in relation to the soil's infiltration and drainage abilities and under-estimate soil saturation and drainage intensities in lower intensity storms where infiltration excess is not triggered. This may alter our understanding of the system's ecology and soil water relationships. It may also influence our ability to predict the leaching of agrichemicals causing possible over-predictions in high intensity

storms and under predictions in low intensity storms. The study illustrates how predicting the dominant surface runoff mechanism can depend on the rainfall resolution. Temporally averaged high intensity storms are more likely to produce saturation excess surface runoff, whereas high resolution rainfall is more likely to produce a larger amount of infiltration excess runoff. These differences in runoff mechanisms create differences in the dynamics of surface runoff, with infiltration excess being more intense and for shorter periods of time than saturation excess. The impacts of these differences in point scale dynamics on larger scale predictions are uncertain and will depend on hillslope properties. This paper highlights how rainfall resolution impacts point scale surface runoff predictions and that if we are not accurately representing point scale processes how can we expect to understand and predict runoff at larger scales?

Acknowledgements. The authors would like to acknowledge financial support from The Minerals and Energy Research Institute Western Australia and the Charles and Annie Neumann Scholarship scheme of the Faculty of Natural and Agricultural Sciences at The University of Western Australia. We would also like to acknowledge the Bureau of Meteorology, Australian Government for providing one min rainfall data and thanks to B. Kowald from the Climate and Consulting services in Perth for his time and help. Thanks also go to I. Foster and P. Hanson at the Department of Agriculture and Food, Western Australia for also providing one min rainfall data. The authors would also like to express their thanks to M. Trefry and G. McGrath for advice on mathematical coding.

Edited by: M. Sivapalan

References

Beven, K.: Runoff generation in semi-arid areas, Chapter 3, in: Dryland Rivers, Hydrology and geomorphology of semi-arid channels, edited by: Bull, L. J. and Kirkby, M. J., John Wiley and Sons Ltd, Sussex, England, 2002.

Brooks, R. H. and Corey, A. T.: Hydraulic properties of porous media, Hydrology Paper 3, Colorado State University, Fort Collins, CO, 27110, 1964.

Bronstert, A. and Bardossy, A.: Uncertainty of runoff modelling at the hillslope scale due to temporal variations of rainfall intensity, Phys. Chem. Earth, 28, 283–288, 2003.

Cammeraat, E. L. H.: Scale dependent thresholds in hydrological and erosion response of a semi-arid catchment in southeast Spain, Agric., Ecosyst. Environ., 104, 317–332, 2004.

Farmer, D., Sivapalan, M., and Jothityangkoon, C.: Climate, soil and vegetation controls upon the variability of water balance in temperate and semiarid landscapes: Downward approach to water balance analysis, Water Resour. Res., 39(2), 1035–1055, 2003.

Harris, D., Menabde, M., Seed, A., and Austin, G.: Breakdown coefficients and scaling properties of rain fields, Nonlin. Processes Geophys., 5, 93–104, 1998, http://www.nonlin-processes-geophys.net/5/93/1998/.

Hipsey, M. R., Sivapalan, M., and Menabde, M.: A risk-based approach to the design of rural water supply catchments across Western Australia, Hydrol. Sci., 48(5), 709–727, 2003.

Horton, R. E.: The role of infiltration in the hydrological cycle, Transact. Amer. Geophys. Union, 14, 446–460, 1933.

Kirkby, M. J., Bracken, L. J., and Shannon, J.: The influence of rainfall distribution and morphological factors on runoff delivery from dryland catchments in SE Spain, Catena, 62, 136–156, 2005.

Kirkby, M. J. and Cox, N. J.: A climatic index for soil erosion potential (CSEP) including seasonal and vegetation factors, Catena, 25, 333–352, 1995.

Lovejoy, S. and Schertzer, D.: Multifractals, cloud radiances and rain, J. Hydrol., 322, 59–88, 2005.

Menabde, M. and Sivapalan, M.: Modeling of rainfall time series and extremes using bounded random cascades and Levy-stable distributions, Water Resour. Res., 36(11), 3293–3300, 2000.

Menabde, M., Harris, D., Seed, A., Austin, G., and Stow, D.: Multiscaling properties of rainfall and bounded random cascades, Water Resour. Res., 33(12), 2823–2830, 1997.

Mertens, J., Raes, D., and Feyen, J.: Incorporating rainfall intensity into daily rainfall records for simulating runoff and infiltration into soil profiles, Hydrol. Processes, 16, 731–739, 2002.

Milly, P. C. D.: Climate, interseasonal storage of soil water and the annual water balance, Adv. Water Resour., 17, 19–24, 1994.

Over, T. M. and Gupta, V. K.: A space-time theory of mesoscale rainfall using random cascades, J. Geophys. Res., 101, 26 319–26 331, 1996.

Potter, N. J., Zhang, L., Milly, P. C. D., McMahon, T. A., and Jakeman, A. J.: Effects of rainfall seasonality on soil moisture capacity on mean annual water balance for Australian catchments, Water Resour. Res., 41, W06007, doi:10.1029/2004WR003697, 2005.

Puigdefabregas, J., Sole, A., Barrio, G., and Boer, M.: Scales and processes of water and sediment redistribution in drylands: Results from the Rambla Honda field site in Southeast Spain, Earth Sci. Rev., 48, 39–70, 1999.

Rawls, W. J., Ahuga, L. R., and Brakensiek, D. L.: Estimating soil hydraulic properties from soils data, in: Indirect Methods for Estimating the Hydraulic Properties of Unsaturated Soils, edited by: van Genuchten, M. T., Leij, F. J., and Lund, L. J., University of California, Riverside, California, pp. 329–340, 1992.

Reaney, S. M., Bracken, L. J., and Kirkby, M. J.: Use of the conncectivity of runoff model (CRUM) to investigate the influence of storm characteristics on runoff generation and connectivity in semi-arid areas, Hydrol. Processes, [online] doi:10.1002/hyp.6281, 2007.

Singh, V. P.: Effect of spatial and temporal variability in rainfall and watershed characteristics on stream flow hydrographs, Hydrol. Processes, 11, 1649–1669, 1997.

Stomph, T. J., de Ridder, N., Steenhuis, T. S., and van de Giesen, N. C.: Scale effects of Hortonian overland flow and rainfall-runoff dynamics: Laboratory validation of a process-based model, Earth Surface Processes and Landforms, 27, 847–855, 2002.

Struthers, I., Sivapalan, M., and Hinz, C.: A multiple wetting front gravitational infiltration and redistribution model for water balance applications, Water Resour. Res., 42(6), W06406, doi:10.1029/2005WR004645, 2006.

Struthers, I., Sivapalan, M., and Hinz, C.: Conceptual examination of climate-soil controls upon rainfall partitioning in an open-fractured soil I: Single storm response, Adv. Water Resour., 30, 505–517, 2007a.

Struthers, I., Hinz, C., and Sivapalan, M.: Conceptual examination of climate-soil controls upon rainfall partitioning in an open-fractured soil II: Response to a population of storms, Adv. Water Resour., 30, 518–527, 2007b.

Wainwright, J. and Parsons, A. J.: The effect of temporal variations in rainfall on scale dependency in runoff coefficients, Water Resour. Res., 38(12), 1271–1281, 2002.

Wolfram Research Inc.: Mathematica, Version 5.2, Champaign, Illinois, 2005.

Woods, R.: The relative roles of climate, soil, vegetation and topography in determining seasonal and long-term catchment dynamics, Adv. Water Resour., 26, 295–309, 2003.

Woolhiser, D. A. and Goodrich, D. C.: Effect of storm rainfall intensity patterns on surface runoff, J. Hydrol., 102, 335–354, 1988.

Veneziano, D., Bras, R. L., and Nuiemann, J. D.: Nonlinearity and self-similarity of rainfall in time and a stochastic model, J. Geophys. Res., 101, 26 371–26 392, 1996.

Yu, B.: A comparison of the Green-Ampt and a spatially variable infiltration model for natural storm events, Transact. ASAE, 42(2), 89–97, 1999.

Yu, B., Rose, C. W., Coughlan, K. J., and Fentie, B.: Plot-scale rainfall-runoff characteristics and modelling at six sites in Australia and southeast Asia, Transact. ASAE, 40(5), 1295–1303, 1997.